

Effect of the air on the drift velocity of water waves

By JAN ERIK WEBER¹ AND EVEN FØRLAND²

¹Institute of Geophysics, University of Oslo, P.O. Box 1022 Blindern, N-0315 Oslo 3, Norway

²Statoil, P.O. Box 300, N-4001 Stavanger, Norway

(Received 23 May 1989 and in revised form 7 March 1990)

Mean drift currents due to damped, progressive, capillary-gravity waves at an air/water interface are investigated theoretically. The analysis is based on a Lagrangian description of motion. Both media are assumed to be semi-infinite, viscous, homogeneous fluids. The system rotates about the vertical axis with a constant angular velocity $\frac{1}{2}f$, where f is the Coriolis parameter. Owing to viscous effects, the wave field attenuates in time or space. Linear analysis verifies the temporal decay rate reported by Dore (1978*a*). The nonlinear drift velocities are obtained by a series expansion of the solutions to second order in a parameter ϵ , which essentially is proportional to the wave steepness. The effect of the air on the drift current in the water is shown to depend on the values of the frequency ω , wavenumber k , density ρ , and kinematic viscosity ν through *one single* dimensionless parameter Q defined by

$$Q = \frac{\rho_1}{\rho_2} \left[\frac{\omega \nu_1}{2k^2 \nu_2^2} \right]^{\frac{1}{2}},$$

where subscripts 1 and 2 refer to the air and the water, respectively. Dynamically, the increased shear near the interface due to the presence of the air leads to a higher value of the virtual wave stress (Longuet-Higgins 1969). This yields a tendency towards a higher (Eulerian) mean drift velocity as compared to the free-surface case. For temporally damped waves, this stress, due to increased damping, effectively acts over a shorter period of time. Accordingly, the mean current associated with such waves tends to be larger for short times and smaller for large times than that obtained with a vacuum above the water. For spatially damped waves, the virtual wave stress becomes independent of time. The Coriolis force is then needed to balance the wave stress in order to avoid infinitely large drift velocities as $t \rightarrow \infty$. Furthermore, assessment of realistic values for the turbulent eddy viscosities in the air and the ocean is shown to bring the results closer to those obtained for a vacuum/water system.

1. Introduction

Although several attempts had been made to extend the theory by Stokes (1847) on wave drift to include the effect of viscosity, real progress in the field had to await the work of Longuet-Higgins (1953). Longuet-Higgins demonstrated that second-order mean vorticity would be generated in the viscous boundary layer at the surface. This vorticity would diffuse inward, inducing a non-zero mean Eulerian current in the interior of the fluid.

The induced mean vorticity can be associated with an equivalent 'virtual wave stress' (Longuet-Higgins 1969). The magnitude of this stress, being proportional to the mean Eulerian velocity gradient, depends on the physical conditions at the

surface. For an uncontaminated surface, Longuet-Higgins showed that the induced mean velocity gradient at the boundary of the inviscid region initially was equal to that obtained from inviscid theory. Hence, the total mean Lagrangian velocity gradient here was exactly twice that obtained from Stokes' solution. Utilizing a Lagrangian approach *ab initio*, Weber (1983*a*) demonstrated that the virtual wave stress of Longuet-Higgins could be evaluated exactly at the free surface. The notion 'free surface' is here used for an uncontaminated vacuum/water interface. This problem has also been studied by Grimshaw (1981), utilizing the generalized Lagrangian-mean formalism introduced by Andrews & McIntyre (1978).

If the surface is contaminated, i.e. covered by a thin, insoluble film, the situation changes. For the particular case of a tangentially inextensible film, Craik (1982) demonstrated that the generation of vorticity was greatly enhanced, leading to much larger Eulerian drift velocities in the interior. For temporally attenuated waves also, however, the attenuation rate is very much increased. Consequently, the increased virtual wave stress acts over a shorter period of time. Weber & Førland (1989) have shown that, for short capillary-gravity waves, the resulting drift current does not differ dramatically from that obtained when the surface is free.

Dore (1978*a, b*) took into account the fact that the air above the water was viscous, when calculating the drift current. He applied a boundary-layer technique, looking for similarity solutions. Neither temporal nor spatial attenuation were considered. Furthermore, the effect of rotation on the mean flow was neglected. In particular, we find that Dore's drift solution increases without bounds as one moves away from the wave generating area.

Analogous to the case of a surface film, the presence of the air increases the generation of second-order Eulerian vorticity near the ocean surface. The effect is much weaker, though, since the particle motion in the water is less constrained by contact with the air at the sea surface than by the presence of a tangentially inextensible film. Again, the increased effect of viscosity which leads to a larger vorticity generation, also causes the wave field (and the vorticity at the surface) to attenuate more rapidly in time. This will limit the growth of the Eulerian mean current. Spatially damped waves are also considered. Here the virtual wave stress becomes independent of time. Unless the Coriolis force is taken into account, the Eulerian mean current now will increase without limits as $t \rightarrow \infty$.

The development of the drift current is investigated in detail in the present paper. It seems reasonable, particularly for larger values of the wavelength, to use turbulent eddy values for the kinematic viscosities in the air and in the ocean. The introduction of such values is very important as far as quantitative estimates of the drift velocity are concerned.

2. Formulation of the problem

The mathematical formulation follows closely that of Weber (1983*a*; hereinafter referred to as (I)). We now consider monochromatic waves propagating along the uncontaminated interface of two semi-infinite, homogeneous, incompressible fluids. The system is stably stratified with densities ρ_1 and ρ_2 , where subscripts 1 and 2 refer to the upper and the lower layer, respectively. We intend to model an air/water system, so throughout the analysis we assume that $\rho_1 \ll \rho_2$. The whole system rotates about the vertical axis with constant angular velocity $\frac{1}{2}f$, where f is the Coriolis parameter.

The mathematical description of the fluid motion will be Lagrangian, and the dependent variables of the problem are expressed as functions of the Lagrangian coordinates (a, b, c) and time t . A Cartesian right-handed coordinate system is defined such that the (x, y) -axes are situated at the undisturbed interface. The z -axis is directed vertically upwards, and the position of the interface is governed by $c = 0$ for all times. The displacements (x, y, z) and pressure p are written as series expansions after an ordering parameter ϵ , which is essentially proportional to the wave slope (Pierson 1962).

We look at waves propagating along the x -axis with frequency ω and wavenumber k . For the capillary-gravity waves considered here, $\omega \gg f$. Hence the effect of rotation can be neglected in the calculation of the primary wave field. It should be noted that this assumption leads to an incorrect solution for the mean Lagrangian mass transport if an Eulerian description of motion is used. For an inviscid fluid with a free surface this has been demonstrated by Hasselmann (1970). However, by using a Lagrangian formalism from the outset, Weber (1989) shows for a viscous ocean that the effect of the Earth's rotation on the wave field may be safely neglected when $\omega \gg f$, as far as the mean mass transport is concerned.

First, we assume that the wave field attenuates in time owing to the effect of friction. Following Lamb (1932) or (I), the solutions to $O(\epsilon)$ may be written

$$x_{1,2}^{(1)} = -\frac{k}{n} [iA_{1,2} e^{\mp kc} \mp \frac{1}{k} m_{1,2} B_{1,2} e^{\mp m_{1,2}c}] e^{ika+nt}, \quad (2.1)$$

$$z_{1,2}^{(1)} = \frac{k}{n} [\pm A_{1,2} e^{\mp kc} + iB_{1,2} e^{\mp m_{1,2}c}] e^{ika+nt}, \quad (2.2)$$

$$p_{1,2}^{(1)} = \frac{\rho_{1,2}}{n} [(n^2 \mp gk) A_{1,2} e^{\mp kc} - igk B_{1,2} e^{\mp m_{1,2}c}] e^{ika+nt}. \quad (2.3)$$

Here the upper sign corresponds to the upper layer (subscript 1), and the lower sign to the lower layer (subscript 2). The superscripts on the left-hand side denote order of perturbation. Furthermore,

$$m_{1,2}^2 = k^2 + n/\nu_{1,2}, \quad (2.4)$$

where ν is the kinematic viscosity coefficient. This is taken to be constant. To simulate turbulence, the value of ν is allowed to exceed the molecular value, see §6. The wavenumber k is taken to be real. For the time dependence, we assume

$$n = -i\omega - \beta, \quad (2.5)$$

where the frequency ω and the attenuation coefficient β both are real. If $\nu_{1,2}$ are small, one obtains approximately

$$m_{1,2} = (1-i) \left[\frac{\omega}{2\nu_{1,2}} \right]^{\frac{1}{2}} \equiv (1-i) \gamma_{1,2}. \quad (2.6)$$

As mentioned before, we here study ocean surface waves. Hence $\rho_1 \ll \rho_2$. Owing to the relatively small viscosities of air and water, the thickness δ of the viscous boundary layer at each side of the interface is much smaller than the wavelength, i.e. in dimensionless form

$$\delta_{1,2} \equiv \frac{k}{\gamma_{1,2}} \ll 1, \quad (2.7)$$

where $\gamma_{1,2}$ is defined by (2.6). Furthermore, we define a dimensionless parameter θ by

$$\theta \equiv \frac{\rho_1}{\rho_2} \left[\frac{\nu_1}{\nu_2} \right]^{\frac{1}{2}}. \quad (2.8)$$

This parameter appears when we equate the tangential stresses at the air/water interface. Now $(\nu_1/\nu_2)^{\frac{1}{2}}$ is of order unity for an air/water system. Hence

$$\theta \ll 1. \quad (2.9)$$

The coefficients $A_{1,2}$ and $B_{1,2}$ in (2.1)–(2.3) are determined from the linearized boundary conditions at the interface. Here continuity of velocities requires

$$\Delta x_t^{(1)} = 0, \quad c = 0, \quad (2.10)$$

$$\Delta z_t^{(1)} = 0, \quad c = 0, \quad (2.11)$$

where Δ denotes the difference between air and water values across the interface. For the stresses in the fluids, we obtain in the x - and z -directions, respectively:

$$\Delta[\mu(x_{tc}^{(1)} + z_{ta}^{(1)})] = 0, \quad c = 0, \quad (2.12)$$

$$\Delta[-p^{(1)} + 2\mu z_{tc}^{(1)}] = -Tz_{2aa}^{(1)}, \quad c = 0. \quad (2.13)$$

Here $\mu = \rho\nu$ is the dynamic coefficient of viscosity, and T the surface tension at the uncontaminated air/water interface. Subscripts a , c and t denote partial differentiation with respect to space and time, respectively.

Utilizing the relations (2.7) and (2.9), the coefficients $A_{1,2}$ and $B_{1,2}$, obtained from (2.10)–(2.12), may be written as series expansions in the small parameters $\delta_{1,2}$ and θ . For a normalized solution we find, to leading order,

$$\left. \begin{aligned} A_1 &= -1 - (1+i)\delta_1 + \dots, \\ B_1 &= (1-i)\delta_1 + \delta_1^2 - \delta_1\delta_2 - (1-i)\theta\delta_1 + \dots, \\ A_2 &= 1 + \dots, \\ B_2 &= \delta_2^2 + (1-i)\theta\delta_2 + \dots \end{aligned} \right\} \quad (2.14)$$

Finally, by utilizing (2.13), the frequency and the attenuation rate are determined. Defining ω_0 by

$$\omega_0^2 = \left(\frac{\rho_2 - \rho_1}{\rho_2 + \rho_1} \right) gk + \frac{Tk^3}{\rho_2 + \rho_1}, \quad (2.15)$$

we obtain

$$\omega = \omega_0(1 - \theta\delta_2) \quad (2.16)$$

and

$$\beta = \omega(\theta + \delta_2)\delta_2 = 2k^2\nu_2(1 + Q). \quad (2.17)$$

Here Q is defined by

$$Q = \frac{\theta}{\delta_2} = \frac{\rho_1}{\rho_2} \left[\frac{\omega\nu_1}{2k^2\nu_2^2} \right]^{\frac{1}{2}}. \quad (2.18)$$

This parameter yields the increase of the damping rate due to the viscous effect of the air above the water. For $\rho_1 = 0$, i.e. a free surface, (2.17) reduces to the familiar expression for the attenuation coefficient first obtained by Basset (1888). For molecular values of the viscosities in the air and the water, the value of Q ranges from 0.05 to 44 for wavelengths from 1 cm to 10^4 cm. However, at least for longer waves,

the ocean (and the atmosphere) definitely must be regarded as turbulent. This may lead to a considerable decrease of Q , compared to the molecular value. The decrease is basically associated with a larger value of δ_2 in (2.18). We shall return to this problem in §6.

The result (2.17) for the damping rate confirms the calculation by Dore (1978*a*, eqn. (3.13)). Here we have included the effect of capillarity. The modification (2.16) of the inviscid frequency has not been reported before.

We denote the initial wave amplitude by ζ_0 . Insertion to lowest order in the vertical displacements at the interface then yields for the ordering parameter:

$$\epsilon = \zeta_0 \omega/k \tag{2.19}$$

as in (I). If the governing equations were non-dimensionalized, scaling the perturbation displacements and velocities by ζ_0 and $\zeta_0 \omega$, respectively, the equivalent non-dimensional expansion parameter would be the wave steepness $\zeta_0 k$. This is assumed to be a small quantity in our analysis, and we shall not pursue the calculations beyond $O(\zeta_0^2 k^2)$.

3. Equations for the mean current

The problem to $O(\epsilon^2)$ is analogous to that described in (I). We may then write for the mean horizontal flow in each layer:

$$\begin{aligned} \nu \nabla_L^2 \bar{x}_i^{(2)} - \bar{x}_{ii}^{(2)} + f \bar{y}_i^{(2)} = & -\frac{1}{\rho} \overline{p_a^{(1)} x_a^{(1)}} - \frac{1}{\rho} \overline{p_c^{(1)} z_a^{(1)}} + \nu [2 \overline{x_a^{(1)} x_{iaa}^{(1)}} \\ & + 2 \overline{z_c^{(1)} x_{icc}^{(1)}} + 2 \overline{z_a^{(1)} x_{iac}^{(1)}} + 2 \overline{x_c^{(1)} x_{iac}^{(1)}} \\ & + \overline{x_{ia}^{(1)} \nabla_L^2 x^{(1)}} + \overline{x_{ic}^{(1)} \nabla_L^2 z^{(1)}}] + \bar{\Pi}_a^{(2)}, \end{aligned} \tag{3.1}$$

$$\nu \nabla_L^2 \bar{y}_i^{(2)} - \bar{y}_{ii}^{(2)} - f \bar{x}_i^{(2)} = 0, \tag{3.2}$$

where $\nabla_L^2 = \partial^2/\partial a^2 + \partial^2/\partial c^2$. Here we have defined $\Pi^{(2)} = p^{(2)}/\rho + gz^{(2)}$, which constitutes the effective pressure per unit density. The equations for the mean vertical motion are not stated here: the reader is referred to Weber (1987).

The overbars in these equations denote an average over one wave cycle. It is here implicitly assumed that the damping is weak, so that the amplitude reduction over one wave cycle is small. This means that $\beta/\omega \ll 1$ for time damping, where β is given by (2.17). For spatial attenuation, considered in §7, the equivalent expression is $\alpha/k \ll 1$, where α is given by (7.1).

It is natural to compare our calculated currents with Stokes' result for an inviscid fluid (Stokes 1847). We therefore introduce Stokes' surface velocity ($= \zeta_0^2 \omega k$) as a measure of the strength of the currents. Accordingly, we define non-dimensional drift velocities (u, v) in each layer by

$$(u, v) = \frac{\omega}{k^3} (\bar{x}_i^{(2)}, \bar{y}_i^{(2)}). \tag{3.3}$$

We shall assume that there are no mean external pressure gradients to $O(\epsilon^2)$ in this problem, which seems to be a reasonable assumption for a laterally unlimited air/water system. For temporal damping, then, $\bar{\Pi}_a^{(2)} = 0$. Introducing complex drift

velocities by $W_{1,2} = u_{1,2} + iv_{1,2}$, equations (3.1) and (3.2) yield for the upper and lower layer, respectively,

$$\nu_1 W_{1cc} - W_{1t} - ifW_1 = 4k^2\nu_1 e^{-2\beta t}[(1 + (1 + Q)(\gamma_1/\gamma_2)^2) e^{-2kc} - 2(\gamma_1/k)^2 e^{-\gamma_1 c} \sin \gamma_1 c + 3(\gamma_1/k)^2 e^{-2\gamma_1 c}], \quad (3.4)$$

$$\nu_2 W_{2cc} - W_{2t} - ifW_2 = 4k^2\nu_2 e^{-2\beta t}[(2 + Q) e^{2kc} - (\gamma_2/k) e^{\gamma_2 c} (\cos \gamma_2 c - \sin \gamma_2 c) + 2Q(\gamma_2/k) e^{\gamma_2 c} \sin \gamma_2 c], \quad (3.5)$$

where $\gamma_{1,2}$, β and Q are defined by (2.6), (2.17) and (2.18).

At the interface, continuity of the mean horizontal velocities requires

$$\Delta W = 0, \quad c = 0. \quad (3.6)$$

For the mean viscous stresses at the interface, the boundary condition must be considered with some care. Denoting the mean horizontal stress to $O(\epsilon^2)$ in each fluid by $\bar{\tau}_x^{(2)}$ and $\bar{\tau}_y^{(2)}$, we obtain at the interface

$$\Delta \bar{\tau}_x^{(2)} = T \overline{z_{2aa}^{(1)} z_{2a}^{(1)}}, \quad c = 0, \quad (3.7)$$

$$\Delta \bar{\tau}_y^{(2)} = 0, \quad c = 0, \quad (3.8)$$

where

$$\bar{\tau}_x^{(2)} = \mu [\overline{x_{tc}^{(2)}} + \overline{z_{ta}^{(2)}} + \overline{x_{tc}^{(1)} x_a^{(1)}} - \overline{x_{ta}^{(1)} x_c^{(1)}} + \overline{z_{ta}^{(1)} z_c^{(1)}} - \overline{z_{tc}^{(1)} z_a^{(1)}} - 2\overline{x_{ta}^{(1)} z_a^{(1)}}] + \overline{p^{(1)} z_a^{(1)}}, \quad c = 0, \quad (3.9)$$

$$\bar{\tau}_y^{(2)} = \mu \overline{y_{tc}^{(2)}}, \quad c = 0. \quad (3.10)$$

We note that $\overline{z_{ta}^{(2)}}$ and $\overline{z_{2aa}^{(1)} z_{2a}^{(1)}}$ are very small in our problem (for temporal attenuation they vanish identically). Evaluation of (3.7) and (3.8) to sufficient accuracy in the small parameters $\delta_{1,2}$ and θ , yields

$$\Delta(\mu W_c) = 0, \quad c = 0. \quad (3.11)$$

If we neglect the effect of the air, (3.11) reduces to $W_{2c} = 0$ at $c = 0$, as in (I); see also Longuet-Higgins (1953). At infinity, we require:

$$W_1 \rightarrow 0, \quad c \rightarrow \infty, \quad (3.12)$$

$$W_2 \rightarrow 0, \quad c \rightarrow -\infty. \quad (3.13)$$

4. Method of solution

It is straightforward to obtain a pair of particular solutions to the equations (3.4) and (3.5). Using superscript (p) for these solutions, we find

$$W_1^{(p)} = [F_1 e^{-2kc} - 4e^{-\gamma_1 c} \cos \gamma_1 c + 3e^{-2\gamma_1 c}] e^{-2\beta t}, \quad (4.1)$$

$$W_2^{(p)} = [F_2 e^{2kc} - (2k/\gamma_2) e^{\gamma_2 c} (\cos \gamma_2 c + \sin \gamma_2 c) - (4Qk/\gamma_2) e^{\gamma_2 c} \cos \gamma_2 c] e^{-2\beta t}, \quad (4.2)$$

where

$$\left. \begin{aligned} F_1 &= \left[1 - \frac{if}{4k^2\nu_2(1 + Q + \gamma_2^2/\gamma_1^2)} \right]^{-1} \\ F_2 &= \left[1 - \frac{if}{4k^2\nu_2(2 + Q)} \right]^{-1} \end{aligned} \right\} \quad (4.3)$$

For a non-rotating ocean ($f = 0$), we note that (4.1) and (4.2) yield the damped version of Stokes' classic solution outside the viscous boundary layers at the interface. This result conforms to that obtained in (I) for a free surface.

If, by chance, (4.1) and (4.2) should happen to satisfy the boundary conditions (3.6) and (3.11), they would essentially represent the complete solutions to the drift problem. In a one-layer model this may occur if the wind stress at the ocean surface is specified in a particular way; see Weber (1983*b*), and also the discussion by Weber & F orland (1989). In the present problem this is not possible, as seen by insertion from (4.1) and (4.2) into (3.6) and (3.11). Accordingly the complete solutions must be written

$$W_{1,2} = W_{1,2}^{(p)} + W_{1,2}^{(h)}, \quad (4.4)$$

where
$$\nu_{1,2} W_{1,2c}^{(h)} - W_{1,2t}^{(h)} - if W_{1,2}^{(h)} = 0. \quad (4.5)$$

From (3.6) and (3.11) we find that the solutions of the homogeneous problem must satisfy the following conditions at the air/water interface:

$$\Delta(W^{(h)}) = -\Delta(W^{(p)}) = (F_2 - F_1 + 1)e^{-2\beta t}, \quad c = 0, \quad (4.6)$$

$$\Delta(\mu W_c^{(h)}) = -\Delta(\mu W_c^{(p)}) = -2k\mu_2(2 + Q - F_2)e^{-2\beta t}, \quad c = 0. \quad (4.7)$$

If, in a non-rotating system, we compare with the Eulerian formulation of Longuet-Higgins (1953), then our part $W^{(p)}$ of the solution, evaluated at $|c| \gg \gamma_{1,2}^{-1}$, corresponds to the inviscid Stokes drift, while $W^{(h)}$ is an approximation to the mean Eulerian drift velocity. This statement has to be slightly modified when rotation is taken into account; see the discussion in §5. A non-zero Eulerian mean current must develop, in Longuet-Higgins' formulation, because the classic Stokes drift alone is unable to match the viscous solution at the outer edge of the boundary layers. Hence the boundary layers, or the surface in a Lagrangian formulation, can be considered as a source of mean secondary vorticity. This will diffuse upwards and downwards and change the original distribution of mean momentum. We note from (4.6) and (4.7) that we have in the present problem *two* independent sources for the redistribution of mean momentum. We shall shortly return to assess their relative importance.

When the wave motion starts it is reasonable to assume that, outside the viscous boundary layers, the classic Stokes solution for the wave drift will be established within a few wave cycles. It is more difficult to assess the initial distribution of mean momentum within the viscous boundary layers. Mathematically, however, contributions from the initial values in these regions only introduce rapidly damped, oscillatory terms. These terms disappear within a wave period, or so, and are therefore unimportant. Accordingly, we take the initial distribution of momentum in the boundary layers to be such as to minimize the number of vanishing transients in the solutions. This happens if we take

$$W_1(t = 0) = e^{-2kc} - 4e^{-\gamma_1 c} \cos \gamma_1 c + 3e^{-2\gamma_1 c}, \quad (4.8)$$

$$W_2(t = 0) = e^{2kc} - (2k/\gamma_2) e^{\gamma_2 c} (\cos \gamma_2 c + \sin \gamma_2 c) - (4kQ/\gamma_2) e^{\gamma_2 c} \cos \gamma_2 c. \quad (4.9)$$

From (4.1), (4.2) and (4.4), we then obtain the following initial conditions for the solutions of the homogeneous problem:

$$W_{1,2}^{(h)}(t = 0) = (1 - F_{1,2}) e^{\mp 2kc}. \quad (4.10)$$

Solutions for the induced motion $W_{1,2}^{(h)}$ are easily obtained by Laplace transforms.

The result is somewhat lengthy, and is therefore placed in the Appendix. However, we shall see that these solutions can be simplified.

From now on we concentrate on the drift current in the water. In particular we focus on the contributions to the mean drift from the 'sources' (4.7) and (4.6). From (A 1) (first integral) these may be written

$$W_2^{(h)} = 2k(\nu_2/\pi)^{\frac{1}{2}} e^{-2\beta t} [E_I + E_{II}] + \dots, \quad (4.11)$$

$$\text{where} \quad E_I = (2 + Q - F_2) \int_0^t \frac{\exp[(2\beta - if)\xi - c^2/(4\nu_2\xi)]}{\xi^{\frac{3}{2}}} d\xi, \quad (4.12)$$

$$E_{II} = \frac{1}{2}c\gamma_2 Q(1 + F_2 - F_1) \int_0^t \frac{\exp[(2\beta - if)\xi - c^2/(4\nu_2\xi)]}{\omega\xi^{\frac{3}{2}}} d\xi. \quad (4.13)$$

We note that E_{II} , which originates from (4.6), is identically zero at the air/water interface $c = 0$. However, it is easy to realize that E_{II} in practice is negligible compared to E_I at all depths. This is basically due to the different behaviour in time of the two integrals in (4.12) and (4.13). Except for very small times, the first integral will always dominate. To demonstrate this quantitatively, we have performed some numerical tests, using molecular kinematic viscosities $\nu_1 = 0.14 \text{ cm}^2 \text{ s}^{-1}$ and $\nu_2 = 0.012 \text{ cm}^2 \text{ s}^{-1}$. We have chosen $c = -1/\gamma_2$, which is just below the surface boundary layer, i.e. before too strong spatial damping in the integrals occur. Varying the wavelength from 1 cm to 10^4 cm, we found that E_I would tend to dominate in (4.11) after 0.1 s for the shortest waves, increasing to about 2 s for the longest. Even for the shortest wave this is a small period of time as far as the development of the drift current is concerned (Weber & Førland 1989, figure 4). At larger depths, where the drift currents are smaller, a longer time will elapse before E_I tends to dominate. However, for all practical purposes, the wave-induced current may be evaluated under the assumption that $|E_I| \gg |E_{II}|$.

If we now return to our original equations, it follows straightaway that making the assumption $|E_I| \gg |E_{II}|$ is equivalent to taking

$$\mu_2 |W_{2c}^{(h)}| \gg \mu_1 |W_{1c}^{(h)}|, \quad c = 0 \quad (4.14)$$

in (4.7). This was also anticipated (without proof) by Dore [1978*a*, equation (4.5)] for an air/water system. We have here justified the use of (4.14) in a much more rigorous manner. Applying (4.14) in the calculations or, formally, letting $|E_I| \gg |E_{II}|$ and $\theta \rightarrow 0$ in (A 1), a complete solution for the non-dimensional wave-induced current in the water may be written

$$\begin{aligned} W_2 = & [F_2 e^{2kc} - (2k/\gamma_2) e^{\gamma_2 c} (\cos \gamma_2 c + \sin \gamma_2 c) - (4Qk/\gamma_2) e^{\gamma_2 c} \cos \gamma_2 c] e^{-2\beta t} \\ & + 2k\nu_2^{\frac{1}{2}} (2 + Q - F_2) e^{-2\beta t} \int_0^t \frac{\exp[(2\beta - if)\xi - c^2/(4\nu_2\xi)]}{(\pi\xi)^{\frac{1}{2}}} d\xi \\ & + 2k\nu_2^{\frac{1}{2}} (1 - F_2) e^{-1ft} \int_0^\infty \frac{\exp(-\xi t) \cos(c\xi^{\frac{1}{2}}/\nu_2^{\frac{1}{2}})}{\pi\xi^{\frac{3}{2}}(\xi + 4k^2\nu_2)} d\xi. \end{aligned} \quad (4.15)$$

It is of considerable interest to compare the drift velocity found here with the result for a free surface, originally obtained by Longuet-Higgins (1953), and derived for a rotating ocean in (I). If we use the same initial conditions for the calculations in (I)

λ (cm)	δ_1	δ_2	Q	β_0 (s ⁻¹)	β (s ⁻¹)
1	0.26	7×10^{-2}	0.05	0.95	1.0
10	7×10^{-2}	2×10^{-2}	0.23	0.95×10^{-2}	1.2×10^{-2}
10 ²	1×10^{-2}	3×10^{-3}	1.7	0.95×10^{-4}	2.6×10^{-4}
10 ³	2×10^{-3}	6×10^{-4}	7.6	0.95×10^{-6}	8.2×10^{-6}
10 ⁴	4×10^{-4}	1×10^{-4}	44	0.95×10^{-8}	4.3×10^{-7}

TABLE 1. Variation of parameters and attenuation rates with wavelength. See the text for details

as we have used here for the lower layer, we find that the non-dimensional wave-induced current in the free surface case may be written

$$\begin{aligned}
 W_0 = & [F_0 e^{2kc} - (2k/\gamma_2) e^{\gamma_2 c} (\cos \gamma_2 c + \sin \gamma_2 c)] e^{-2\beta_0 t} \\
 & + 2k\nu^{\frac{1}{2}}(2 - F_0) e^{-2\beta_0 t} \int_0^t \frac{\exp[(2\beta_0 - if)\xi - c^2/(4\nu_2 \xi)]}{(\pi\xi)^{\frac{1}{2}}} d\xi \\
 & + 2k\nu^{\frac{1}{2}}(1 - F_0) e^{-ift} \int_0^\infty \frac{\exp(-\xi t) \cos(c\xi^{\frac{1}{2}}/\nu_2^{\frac{1}{2}})}{\pi\xi^{\frac{1}{2}}(\xi + 4k^2\nu_2)} d\xi,
 \end{aligned} \tag{4.16}$$

where
$$\beta_0 = 2k^2\nu_2, \quad F_0 = \left[1 - \frac{if}{8k^2\nu_2}\right]^{-1}. \tag{4.17}$$

We then note the very interesting fact that the solutions (4.15) and (4.16) are identical, apart from the parameter Q appearing in the former. This means that $W_2 \rightarrow W_0$ when $Q \rightarrow 0$. Accordingly, the entire effect of the air on the drift velocity of water waves is embedded in Q , defined by (2.18). In the next paragraph the difference between (4.15) and (4.16) will be explored in a quantitative sense.

5. Discussion of solutions

For the present problem we take $\rho_1 = 1.25 \times 10^{-3} \text{ gm cm}^{-3}$ and $\rho_2 = 1 \text{ gm cm}^{-3}$. Furthermore, for the surface tension T at the uncontaminated air/water interface we assume $T/\rho_2 = 74 \text{ cm}^3 \text{ s}^{-1}$. Let us first consider *laminar* motion in the air and in the water. We may then take $\nu_1 = 0.14 \text{ cm}^2 \text{ s}^{-1}$ and $\nu_2 = 0.012 \text{ cm}^2 \text{ s}^{-1}$. It is interesting to see how the values of the dimensionless parameters $\delta_{1,2}$ and Q from (2.7) and (2.18) vary with the wavelength, together with the attenuation rates β_0 and β from (4.17) and (2.7). The results are summarized in table 1. Our analysis assumes that δ_1 and δ_2 are small quantities. This is seen to be very well fulfilled. However, some care must be taken in the capillary wave regime. The parameter θ defined by (2.8), which also is assumed to be small, attains here the value 4×10^{-3} .

As noted by Dore (1978*a, b*), the effect of the air is dominant in the damping coefficient for water waves when the wavelength is larger than a metre, or so. This is also evident from table 1, as seen by the increasing difference between β_0 (vacuum/water) and β (air/water).

When the waves decay, their momentum is transferred to the mean current. For a fluid with a free surface, Longuet-Higgins (1969) pointed out that *this transfer may be achieved through the action of a virtual wave stress, τ_w , at the surface.* This is also

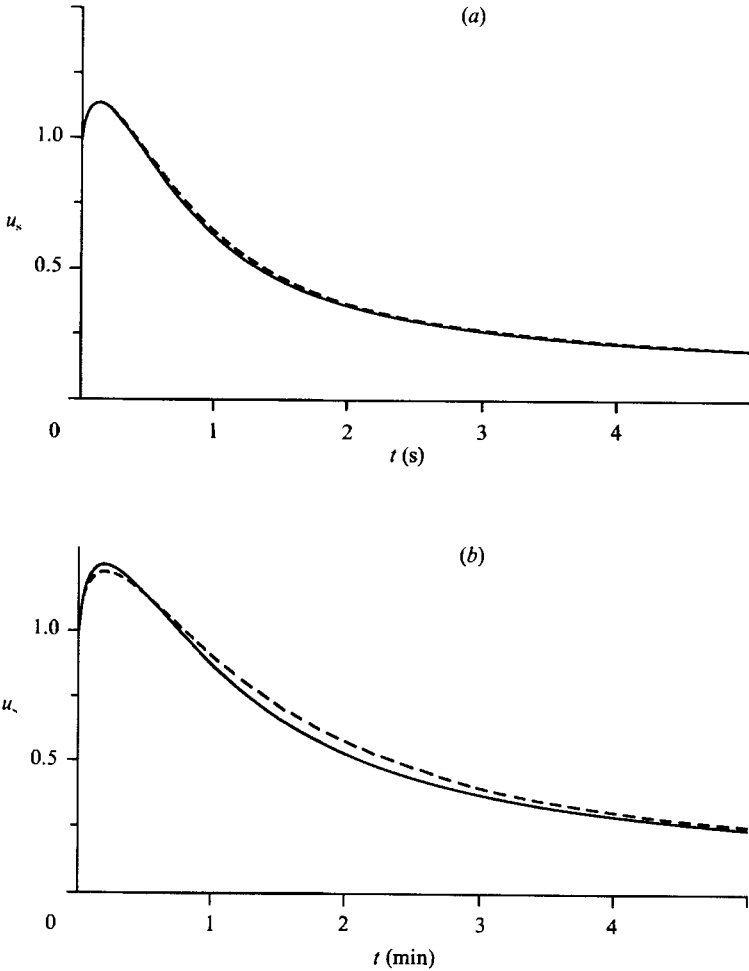


FIGURE 1(a, b). For caption see facing page.

the case for a rotating air/water system, as will be demonstrated below. In order to compare more directly with Longuet-Higgins' results, it proves convenient to make a slight rearrangement of the variables. Accordingly, the mean, non-dimensional velocity in the water, $W_2 (= W_2^{(p)} + W_2^{(h)})$, will now be written

$$W_2 = W_2^{(E)} + [e^{2kc} - (2k/\gamma_2) e^{\gamma_2 c} (\cos \gamma_2 c + \sin \gamma_2 c) - (4Qk/\gamma_2) e^{\gamma_2 c} \cos \gamma_2 c] e^{-2\beta t}. \tag{5.1}$$

Below the vorticity layer, the mean current defined by (5.1) consists of $W_2^{(E)}$ plus the (damped) inviscid Stokes drift. Hence $W_2^{(E)}$ corresponds approximately to the Eulerian mean velocity; although still expressed in Lagrangian coordinates (see also the discussion by Jenkins 1986). Utilizing (4.14), the boundary condition for $W_2^{(E)}$ is obtained from (4.7):

$$W_c^{(E)} = 2k(1+Q) e^{-2\beta t}, \quad c = 0. \tag{5.2}$$

A relevant virtual wave stress for the present problem may then be defined by

$$\tau_w = \rho_2 \nu_2 \zeta_0^2 \omega k W_c^{(E)}, \quad c = 0 \tag{5.3}$$

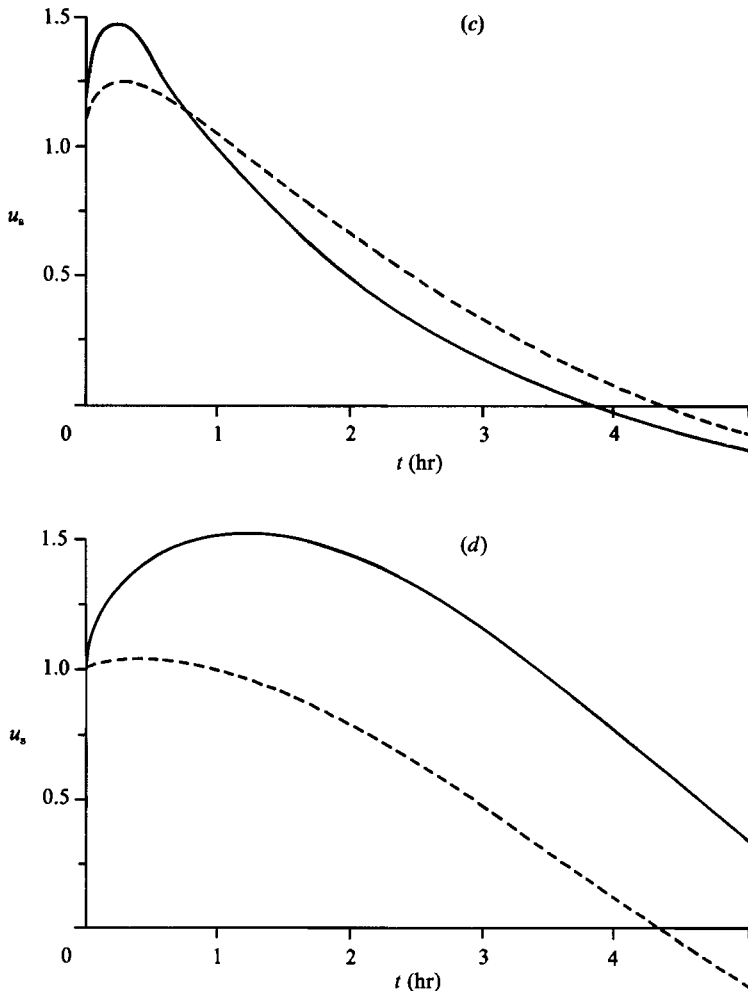


FIGURE 1. Dimensionless surface velocity component $u_s = u(c=0)$ from (4.15) (solid line) and (4.16) (broken line) versus time. Here $\nu_1 = 0.14 \text{ cm}^2 \text{ s}^{-1}$ and $\nu_2 = 0.012 \text{ cm}^2 \text{ s}^{-1}$. (a) $\lambda = 1 \text{ cm}$, (b) $\lambda = 10 \text{ cm}$, (c) $\lambda = 10^2 \text{ cm}$, (d) $\lambda = 10^3 \text{ cm}$. (The *dimensional* velocity scale here is $\zeta_0^2 \omega k$; see the text for meaning of symbols.)

Utilizing this expression, it follows straightaway that

$$\int_0^\infty \tau_w dt = \frac{1}{2} \rho_2 \zeta_0^2 \omega. \quad (5.4)$$

Since $\rho_1 \ll \rho_2$ in the present problem, the left-hand side of (5.4) is equal to the original, total wave momentum of the system. Accordingly, all the momentum is transferred to the mean current by the virtual wave stress, τ_w , defined by (5.3). This is a generalization of the result by Longuet-Higgins (1969) for waves at a free surface in a non-rotating fluid.

From the calculations of Weber & Førlund (1989) for short capillary-gravity waves at a film-covered surface, it is easy to see that the relation (5.4) holds as well. This comes, of course, as no surprise. As pointed out by Longuet-Higgins (1969), this relation must be valid even for breaking waves.

Intuitively one might think that a more rapid wave decay should imply a stronger mean current. However, this argument certainly must be considered with some care. Weber & Førland (1989) demonstrated that for waves at a contaminated surface, the effect of larger damping led to an initially larger value of τ_w . This yields a tendency towards a stronger growth of the drift current for short times. But as time progresses, τ_w itself is subject to stronger decay, which limits the growth of the induced current. At larger times the stronger decrease of τ_w generally leads to a smaller drift current than would have occurred with less damping. Qualitatively the same story is true for an air/water system, but the effect is weaker. This is obvious from figure 1 where we have displayed the dimensionless surface velocity component $u_s = u(c = 0)$ from (4.15) (solid line) and (4.16) (broken line) as functions of time for various values of the wavelength. We have used molecular values for the kinematic viscosities here. For $\lambda = 1$ cm the two results are nearly indistinguishable, as seen from figure 1(a). For larger wavelengths, the results displayed in figure 1(b, c) clearly exhibit a tendency towards larger currents at short times and smaller currents at larger times when the air is present. This is also true for the results plotted in figure 1(d), even if it does not show up within the timescale of the plot. However, although the ratio of the attenuation coefficients, β/β_0 , here may be quite large, the increase in current is seen to be moderate. For $\lambda = 10^3$ cm, we have $\beta/\beta_0 = 8.6$, while from figure 1(d) we note that the ratio of the current maxima is about 1.5.

6. Effect of turbulence

Under realistic conditions turbulence will always be present in the ocean and in the atmosphere. For wind-generated waves observations indicate that the mean current in the turbulent region immediately below the surface varies linearly with depth. Further below the surface, the velocity profile is logarithmic (Shemdin 1972; Wu 1975; McLeish & Putland 1975). This is similar to flow over a flat plate. Assuming that the mean stress also is constant in the constant-shear region (and equal to the surface value τ_s), an effective turbulent eddy viscosity $\nu_2^{(T)}$ may be written (Bye 1988):

$$\nu_2^{(T)} = \frac{\kappa u_{*2}^3}{2Kg} \left[\frac{\rho_2}{\rho_1} \right]. \quad (6.1)$$

Here $\kappa = 0.4$ is von Kármán's constant and $u_{*2} = (\tau_s/\rho_2)^{1/2}$ is the friction velocity in the water. K is obtained from the wave spectrum, and Phillips (1985) estimates that K lies in the range $0.2 \leq K \leq 0.5$. In Bye's formulation the roughness length z_2 in the water is given by

$$z_2 = C_2 u_{*1}^2/g, \quad (6.2)$$

where $u_{*1} = (\tau_s/\rho_1)^{1/2}$ is the friction velocity in the air, and $C_2 = 1/(2K)$.

Assuming that the shear stress is also constant in the logarithmic region, one finds that the eddy viscosity varies linearly with depth. It should be noted, however, that the slopes of the logarithmic velocity profiles obtained by Cheung & Street (1988) deviate from the flat-plate value of u_{*2}/κ for stronger wind speeds. This indicates that the waves may affect the turbulent mean flow directly.

It appears that the turbulent mean flow in the air above the wavy surface is similar to that in the water (Bye 1988). Accordingly, the effective eddy viscosity in the constant-shear layer in the air may be written

$$\nu_1^{(T)} = \kappa u_{*1} z_1. \quad (6.3)$$

Here the roughness length z_1 is given by the empirical relation

$$z_1 = C_1 u_{*1}^2/g, \quad (6.4)$$

where $C_1 = 0.0185$ (Wu 1982).

In the present problem the wind is not directly involved, and the turbulence is a reminiscence of earlier wind events. Furthermore, we neglect the vertical variation of the eddy viscosities. This will affect the drift solutions quantitatively (Madsen 1977; Jenkins 1987). However, it will not alter the basic nature of the problem. To obtain representative order of magnitude estimates for the viscosities in the air and in the water, we consider values in the constant-shear layers at both sides of the air/water interface. A conservative estimate for light winds yields $\nu_2^{(T)} \sim 1 \text{ cm}^2 \text{ s}^{-1}$ in the surface layer. This is consistent with the measurements of Churchill & Csanady (1983). For the effective viscosity in the constant-shear layer at the air side of the interface, we obtain from (6.1)–(6.4):

$$\nu_1^{(T)} = (C_1/C_2) (\rho_2/\rho_1)^{1/2} \nu_2^{(T)}. \quad (6.5)$$

We note that this relation is independent of the surface stress. Here we assume that (6.5) is valid in the absence of wind. Taking $K = 0.35$ (Bye 1988), i.e. $C_2 = 1.4$, we find that $(C_1/C_2) (\rho_2/\rho_1)^{1/2} \approx 0.4$ in (6.5). Hence it seems fair to assume that $\nu_1^{(T)}$ and $\nu_2^{(T)}$ are of the same order of magnitude.

We recall from the discussion of the laminar case in §5 that the effect of the air became increasingly more important for the wave drift as the wavelengths grew longer. This is basically related to the growth of the parameter Q , defined by (2.18). With realistic turbulent values for the viscosities in the air and the ocean, the effect of the air becomes much less pronounced. To illustrate this point, we consider waves with wavelengths 10^3 cm and 10^4 cm , respectively. Taking $\nu_1 = \nu_1^{(T)} = 1 \text{ cm}^2 \text{ s}^{-1}$ and $\nu_2 = \nu_2^{(T)} = 1 \text{ cm}^2 \text{ s}^{-1}$, we find that $Q = 0.22$ and $Q = 1.26$ for these two respective wavelengths. From (2.17) and (4.17) it is then noted that the damping rates are increased by 22% and 126%, respectively, owing to the presence of the air. This increase is very much less than that obtained for waves in a laminar air/water system, as seen from table 1.

In figure 2 we have plotted $u_s = u(c = 0)$ from (4.15) (solid line) and (4.16) (broken line) as functions of time for $\nu_1 = \nu_2 = 1 \text{ cm}^2 \text{ s}^{-1}$. Figure 2(a) depicts the development of this component when $\lambda = 10^3 \text{ cm}$. We note that the former tendency persists, i.e. the effect of the air introduces larger currents at short times and smaller currents at large times. But now the deviation from the results obtained with a free surface (i.e. $\rho_1 = 0$) is almost negligible. Comparison with the case of molecular viscosities (figure 1(d), solid line) further shows that the presence of turbulence in this case increases the damping and reduces the maximum current velocity.

Figure 2(b) portrays the same situation as in figure 2(a), but now with $\lambda = 10^4 \text{ cm}$. Here the free-surface solution (broken line) underestimates the current speed in the entire timescale of the plot (5 hr). However, the deviation from the air-influenced solution is quite small.

Various observations seems to support an order of magnitude estimate of $1 \text{ cm}^2 \text{ s}^{-1}$ for the eddy viscosity in the water for light or vanishing winds. It may be more difficult to assess the appropriate value for the eddy viscosity in the air above the water. Based on the idea that the signature of the wind- and wave-generated turbulence will persist also when the wind has disappeared, the present estimates yield that the eddy viscosity in the air near the ocean surface should be of the same order of magnitude as in the water. Fortunately, however, the magnitude of the wave

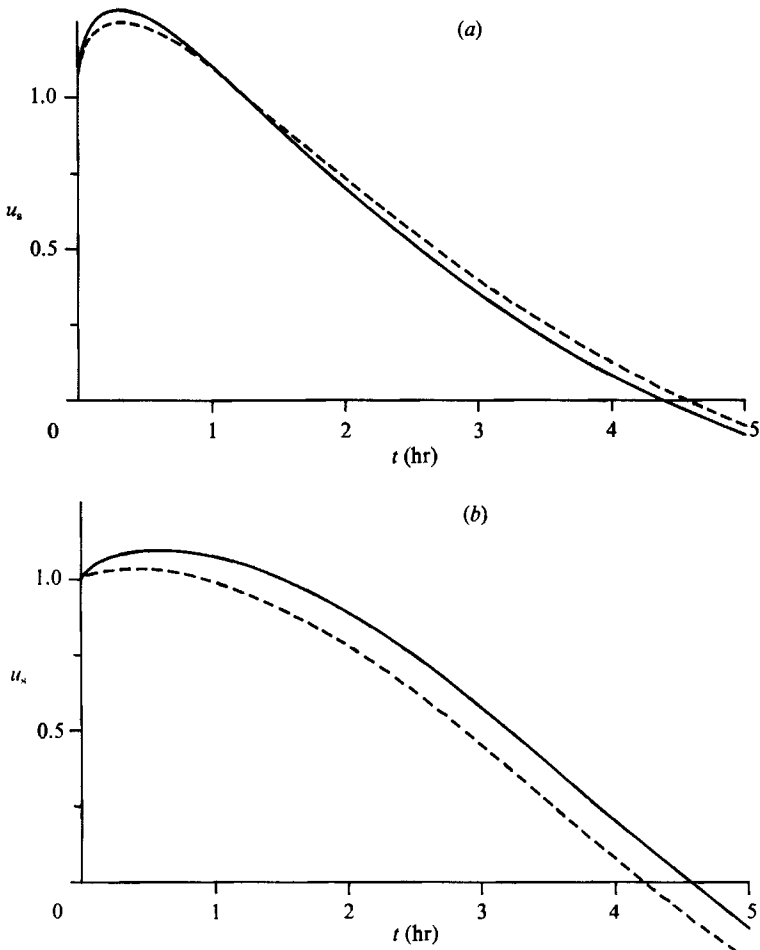


FIGURE 2. Same as in figure 1, but for $\nu_1 = \nu_2 = 1 \text{ cm}^2 \text{ s}^{-1}$: (a) $\lambda = 10^3 \text{ cm}$, (b) $\lambda = 10^4 \text{ cm}$.

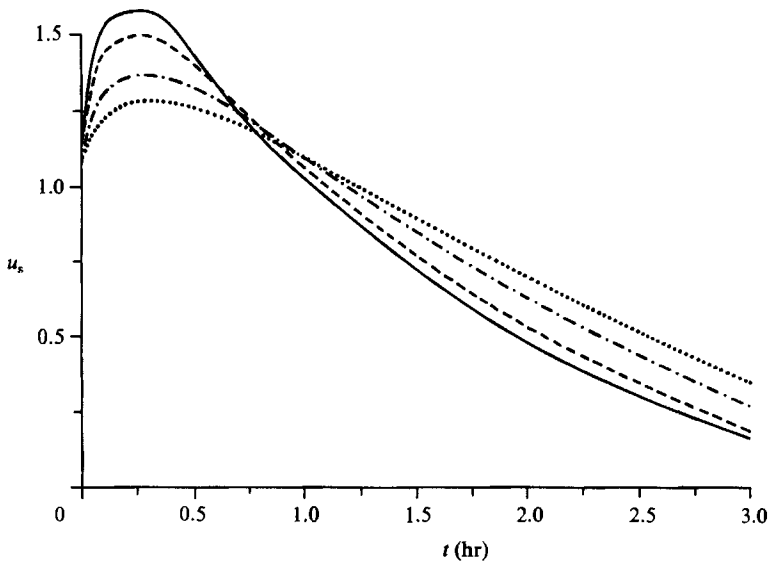


FIGURE 3. Same as in figure 1, but for $\nu_2 = 1 \text{ cm}^2 \text{ s}^{-1}$ and $\lambda = 10^3 \text{ cm}$: \cdots , $\nu_1 = 1 \text{ cm}^2 \text{ s}^{-1}$; $-\cdot-\cdot-$, $\nu_1 = 10 \text{ cm}^2 \text{ s}^{-1}$; $---$, $\nu_1 = 50 \text{ cm}^2 \text{ s}^{-1}$; $---$, $\nu_1 = 100 \text{ cm}^2 \text{ s}^{-1}$.

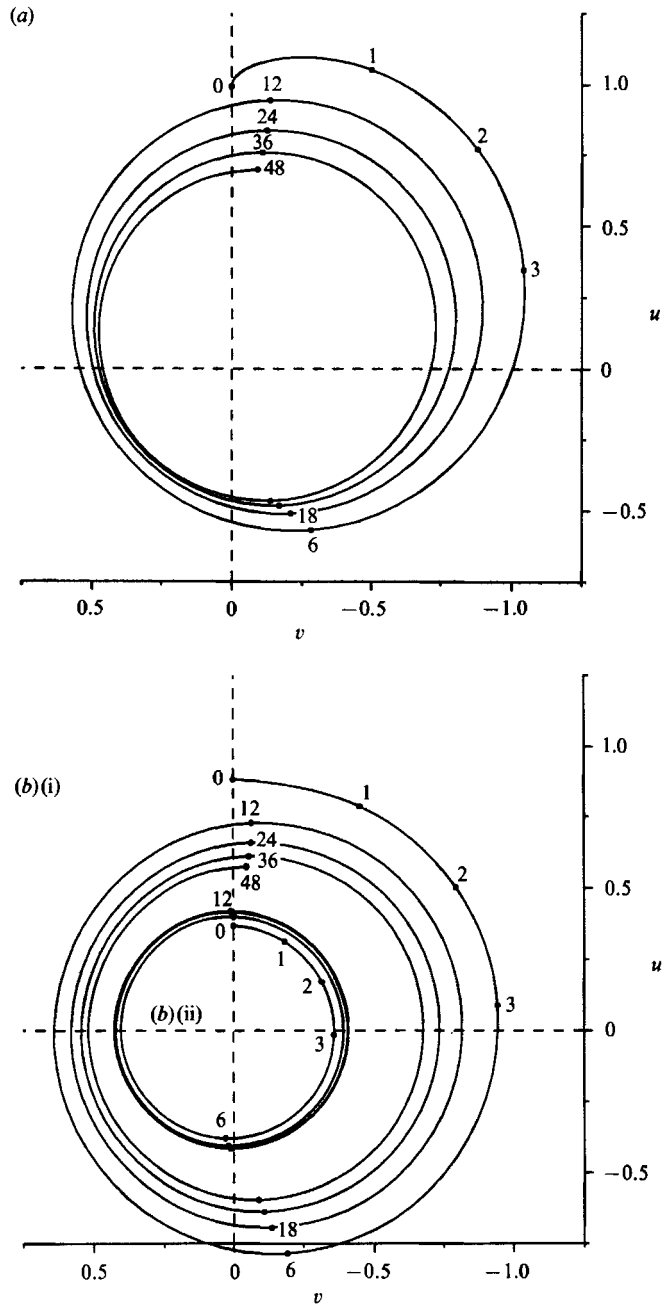


FIGURE 4. Hodograph of the dimensionless drift current (4.15) for temporally damped waves at various depths. The numbered black dots denote evolution time in pendulum hours. Here $\nu_1 = \nu_2 = 1 \text{ cm}^2 \text{ s}^{-1}$ and $\lambda = 10^4 \text{ cm}$. (a) $c = 0$, (b) (i) $c = -10^2 \text{ cm}$, (b) (ii) $c = -8 \times 10^2 \text{ cm}$.

drift current is not very sensitive to changes in ν_1 . This is obvious from figure 3, where we have plotted $u_s = u(c = 0)$ from (4.15) for $\lambda = 10^8 \text{ cm}$ for values of ν_1 increasing by a factor of 100, from $1 \text{ cm}^2 \text{ s}^{-1}$ to $100 \text{ cm}^2 \text{ s}^{-1}$. In these computations the value of ν_2 has been kept fixed ($= 1 \text{ cm}^2 \text{ s}^{-1}$).

For larger times, the effect of the Earth's rotation will affect the solutions. This is

obvious from figure 4 where we have displayed hodographs of the dimensionless wave drift current (4.15) at various depths. In these computations we have taken $\nu_1 = \nu_2 = 1 \text{ cm}^2 \text{ s}^{-1}$ and $\lambda = 10^4 \text{ cm}$. The numbered black dots on the graphs denote evolution time in pendulum hours. For the Coriolis parameter we have chosen $f = 1.2 \times 10^{-4} \text{ s}^{-1}$. The graphs clearly show that the wave drift current contains a pronounced element of inertial oscillations. This is obvious from the observed period of 12 pendulum hours in the plots. Similar results are presented in (I) for a free surface; see also Jenkins (1986) and Weber (1989). If we entirely neglect the effect of viscosity in the air and the water, i.e. $\nu_1 = \nu_2 = 0$, the mean drift currents will be purely inertial, as demonstrated by Hasselmann (1970) and Pollard (1970). The hodographs will then be closed circles centred at the origin. Figure 4(a) displays the surface current for the present case. We note that the inclusion of viscosity induces a net current, when averaged over the inertial period. At the surface this slowly damped net current is directed to the right of the wave propagation direction (the x -axis). The deflection angle is about 45° . At larger depths the net current is veering to the right (on the Northern Hemisphere). An appropriate Ekman depth $D_E = \pi(2\nu_2/f)^{1/2}$ may be defined in the water. For this example $D_E = 4 \times 10^2 \text{ cm}$. Figure 4(b)(i) depicts the drift current at $c = -10^2 \text{ cm}$, i.e. within the upper part of the Ekman layer. We now note that the net current, averaged over one inertial period, is deflected about 90° to the right of the wave propagation direction. Below the Ekman layer, the net current practically vanishes. The motion here is purely inertial. This is obvious from figure 4(b)(ii), which displays the hodograph at $c = -8 \times 10^2 \text{ cm}$. We note a slight increase in the magnitude of the drift current. This increase occurs essentially after 6–12 pendulum hours, and is due to downward diffusion of wave momentum from the surface. Finally, for sufficiently large times, the current spirals in figure 4 will all end up in the origin.

For increasing values of the eddy viscosities, the magnitude of the drift currents become larger for the early hours of the motion, and the subsequent damping of the inertial oscillations become more efficient; see also Weber (1989).

7. Spatial attenuation

For most laboratory tests, the waves are produced by a wave generator operating at a given frequency. Owing to the effect of viscosity, the wavenumber now becomes complex, i.e. the wave amplitude decays exponentially in space. The spatial and temporal attenuation coefficients α and β are related through

$$\alpha = \beta/c_g = 2k^2\nu_2(1+Q)/c_g, \quad (7.1)$$

where c_g is the group velocity of the waves (Gaster 1962). Here $c_g = \omega/(2k)$, while β is obtained from (2.17). Also ocean swell, emanating from a local storm area, may conveniently be described by spatial attenuation. The drift currents due to such waves may readily be obtained from the present calculations. Consider monochromatic, spatially attenuated waves. The particular solution to the non-rotating mean drift equations in Lagrangian form must also now yield the modified Stokes drift. The modification is due to viscosity, and occurs in the thin boundary layers near the air/water interface. This modified Stokes drift is the same as that obtained for temporally damped waves, except that the damping factor $\exp(-2\beta t)$ is replaced by $\exp(-2\alpha a)$. We have here assumed that $a \in [0, \infty)$. The arguments above is easily seen to be valid for the free-surface case (Jenkins 1986). Comparing with the results of Weber (1987) and Weber & Førland (1989), this is also seen to apply when the

surface is covered by a thin ice sheet, or a tangentially inextensible oil film. Accordingly, for an air/water system, the spatially damped analogue to the mean drift equations (3.4) and (3.5) may be written

$$L_1(W_1) = 4k^2\nu_1 e^{-2\alpha a} [e^{-2kc} - 2(\gamma_1/k)^2 e^{-\gamma_1 c} \sin \gamma_1 c + 3(\gamma_1/k)^2 e^{-2\gamma_1 c}], \quad (7.2)$$

$$L_2(W_2) = 4k^2\nu_2 e^{-2\alpha a} [e^{2kc} - (\gamma_2/k) e^{\gamma_2 c} (\cos \gamma_2 c - \sin \gamma_2 c) + 2Q(\gamma_2/k) e^{\gamma_2 c} \sin \gamma_2 c]. \quad (7.3)$$

Here $L_{1,2}$ is the differential operator defined by the right-hand sides of (3.4) and (3.5). We have utilized the fact that $|\partial^2/\partial c^2| \gg |\partial^2/\partial a^2|$ in this case.

It should be noted that the mean horizontal pressure gradient, $\bar{\Pi}_a^{(2)}$ in (3.1), is not zero in this case. Formally, it can be obtained from the equation for the mean vertical motion; see Weber (1987) for a similar problem.

Utilizing the boundary conditions (3.11)–(3.13) and the initial conditions (4.8) and (4.9) for spatially damped waves, the wave drift solutions in the air and the water may be derived in the same manner as before. Again we simplify the problem by utilizing the approximation (4.14). The non-dimensional wave-induced mean current in the water may then be written

$$W_2 = \left[\hat{F}_2 e^{2kc} - (2k/\gamma_2) e^{\gamma_2 c} (\cos \gamma_2 c + \sin \gamma_2 c) - (4Qk/\gamma_2) e^{\gamma_2 c} \cos \gamma_2 c + 2k\nu_2^{\frac{1}{2}} (2 + Q - \hat{F}_2) \int_0^t \frac{\exp[-if\xi - c^2/(4\nu_2\xi)]}{(\pi\xi)^{\frac{1}{2}}} d\xi + 2k\nu_2^{\frac{1}{2}} (1 - \hat{F}_2) e^{-ift} \int_0^\infty \frac{\exp(-\xi t) \cos(c\xi^{\frac{1}{2}}/\nu_2^{\frac{1}{2}})}{\pi\xi^{\frac{1}{2}}(\xi + 4k^2\nu_2)} d\xi \right] e^{-2\alpha a}. \quad (7.4)$$

Here
$$\hat{F}_2 = \left[1 - \frac{if}{4k^2\nu_2} \right]^{-1}. \quad (7.5)$$

Again, this solution reduces to that obtained for a free surface when $Q \rightarrow 0$.

When a wave generator is operated continuously, energy and momentum are supplied to the region $a \in [0, \infty)$ at a constant rate. Accordingly, the virtual wave stress at a specific point becomes independent of time. In a non-rotating system this will lead to drift currents that increase in time. This is easily seen from the solution (7.4). For $f = 0$, we find that $u_s = u(c = 0) \rightarrow \infty$ as $t \rightarrow \infty$. When rotation is taken into account, the wave stress will tend to get balanced by the Coriolis force. Hence a steady state is achieved as $t \rightarrow \infty$.

The wave drift current is also now in general directed to the right of the wave propagation direction (when $f > 0$). At the surface, the deflection angle depends on the dimensionless parameters Q and R , where the latter is defined by

$$R = \left[\frac{f}{8k^2\nu_2} \right]^{\frac{1}{2}}. \quad (7.6)$$

This expresses the ratio between a Stokes depth $1/(2k)$ and an Ekman depth $(2\nu_2/f)^{\frac{1}{2}}$. In terms of R , we obtain two limiting forms of the steady surface current from (7.4):

$$W_s = \frac{1+Q}{2R} (1-i) e^{-2\alpha a}, \quad R \ll 1, \quad (7.7)$$

and
$$W_s = \frac{2+Q}{2R} (1-i) e^{-2\alpha a}, \quad R \gg 1. \quad (7.8)$$

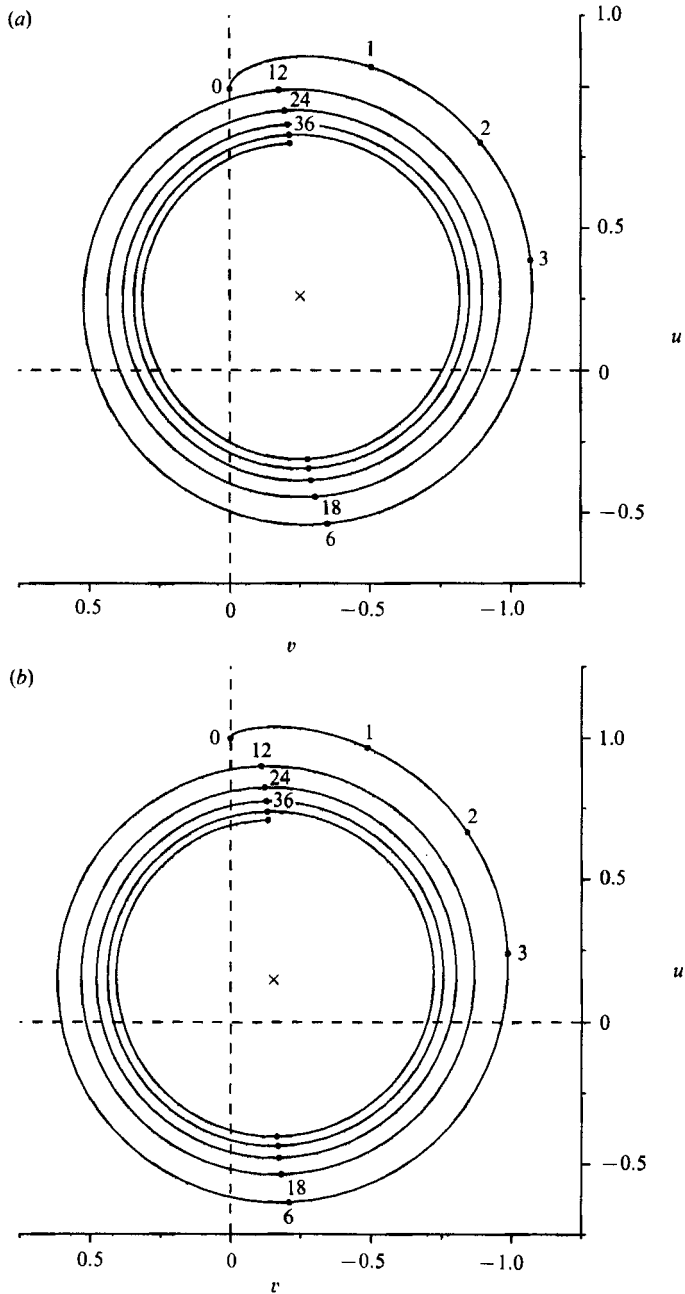


FIGURE 5. Hodograph of the dimensionless surface drift current (7.4) for spatially damped waves. Here $a = 0$, $\nu_1 = \nu_2 = 1 \text{ cm}^2 \text{ s}^{-1}$ and $\lambda = 10^4 \text{ cm}$. Numbered black dots are the same as in figure 4. (a) Effect of air included; (b) free surface ($\rho_1 = 0$).

For both these limits we note that the steady surface current is directed 45° to the right of the wave propagation direction, irrespective of the value of Q . Using our previous values for the turbulent eddy viscosities ($\nu_1 = \nu_2 = 1 \text{ cm}^2 \text{ s}^{-1}$), and taking $f = 1.2 \times 10^{-4} \text{ s}^{-1}$, we find that $R = 6.2$ for waves of wavelength 10^4 cm . The result for the surface current then becomes close to that given by (7.8). In the present example

$Q = 1.25$. Accordingly, the viscous effect of the air increases the current speed at $a = 0$ by about 60%. One should note, however, that the magnitude of the steady current is only slightly more than $\frac{1}{3}$ of the initial Stokes drift in this case. This is also obvious from figure 5, where we have plotted hodographs of the surface current from (7.4). We have taken $a = 0$, and the parameters are those stated above. In figure 5(a) the viscous effect of the air is included, while figure 5(b) depicts the free-surface case ($\rho_1 = 0$). The crosses on the plots denote the steady limit as $t \rightarrow \infty$.

For the current speed away from the wave generation area ($a > 0$), it is important to include the increased spatial damping due to the presence of air. With $Q = 1.25$, we note from (7.1) that the damping coefficient in the present example is more than twice that of a free surface. This relatively stronger spatial damping means that we, beyond a certain distance d from the wave generator, find that the air-influenced drift current becomes *smaller* than its free-surface counterpart. For $R \gg 1$, we obtain from (7.8)

$$d = \frac{\ln(1 + \frac{1}{2}Q)}{4k^2\nu_2 Q/c_g}. \quad (7.9)$$

For the present example we find $d \sim 1.5 \times 10^3$ km. This may be a relevant distance from the coast to a potential generation area for ocean swell.

It is worth remembering that, since the mean drift velocities u_1 and u_2 here have a weak horizontal dependence, continuity requires small vertical mean velocities in both fluids. Denoting these by w_1 and w_2 , respectively, the nonlinear continuity equation in Lagrangian form yields, to $O(\epsilon^2)$,

$$w_{1,2} = 2\alpha \int_0^c u_{1,2} dc. \quad (7.10)$$

We have here assumed that $w_1 = w_2 = 0$ at $c = 0$. Owing to the small value of the attenuation coefficient α , the mean vertical motion discussed here will in practice be negligible.

8. Summary and discussion

Since the density of air is very much less than that of water, the dispersion relation for waves at an air/water interface deviates very little from that obtained by replacing the air by vacuum. However, as pointed out by Dore (1978*a*), the viscous damping of the waves tends to be dominated by the presence of the air, when the wavelength is more than 1 m, or so. Consequently, the nonlinear transfer of momentum from the waves to the mean current will be dominated by the air for longer waves. According to Dore (1978*a, b*), the drift current should then become substantially larger than that obtained from earlier theories (e.g. Longuet-Higgins 1953).

Although Dore's results now have been known for more than 10 years, their implications have not, to the authors' knowledge, been incorporated in common prognostic models for wind- and wave-induced ocean currents. This may have several reasons. First, it is fair to say that it is not easy, neither from laboratory experiments nor from field measurements, to find evidence for substantially larger wave drift currents than those predicted by earlier theories. Secondly, Dore's theory has several weaknesses. In particular, the effects of temporal or spatial damping are not taken into account, and the validity of the solutions are limited to a certain area downstream of the generating region. Furthermore, the effect of the Earth's rotation

is neglected, and no attempt has been made to quantify the effect of turbulence on the mean drift solutions.

Some of these deficiencies are related to the mathematical approach adopted by Dore, i.e. the formulation of a double boundary-layer model where one looks for similarity solutions. We have here chosen a very different theoretical approach to the wave drift problem. In particular we use a Lagrangian description of motion. This has great advantages in problems including oscillating material surfaces, like the air/water interface in this case. The analysis becomes fairly straightforward, with no need for assumptions that limit the solutions in any severe way, as long as the wave steepness stays small.

Our results show that the effect of the air on the mean wave-induced drift current can be incorporated into one single parameter Q , defined by (2.18). We find that the inclusion of the air does not change the drift currents substantially for temporally damped waves. There is, however, a tendency for higher velocities at short times and smaller velocities at large times. Particularly for longer waves, it is important to apply realistic values for the eddy viscosities in the air and the ocean. This is shown to diminish the effect of the air upon the drift current in the water.

The effect of air becomes most pronounced for spatially damped waves. A continuous generation of wave energy now yields a time-independent virtual wave stress at any specific point behind the wave generator. Unless the Earth's rotation is taken into account, the surface current will continue to grow as $t \rightarrow \infty$. In practice, however, and particularly in connection with laboratory experiments, the wave generator will operate only for a limited period of time. This will limit the growth of the current. Unfortunately, we have not been able to find any suitable experimental data relevant to the present problem (deep water, no endwalls, uncontaminated surface). Hence, no comparisons between theory and observations could be made.

For this particular study of capillary-gravity waves along an air/water interface, we have considered monochromatic waves. A generalization to a random wave field is straightforward (Chang 1969; Jenkins 1986). However, such an approach is usually of greatest interest when a wind is blowing, and we have a fully developed sea state. This generalization will therefore be left for future research which includes the combined action of wind and waves.

This research was in part supported by Statoil under contract no. T 7333. Arne Melsom is gratefully acknowledged for his assistance concerning the numerical evaluation and the plotting of the presented results.

Appendix. Induced mean motion

The induced mean motion $W_{1,2}^{(h)}$ in the air and the water is obtained by Laplace-transforming the governing equation (4.5) and the boundary conditions (4.6) and (4.7). The initial values are given by (4.10). Utilizing the shifting and convolution properties of Laplace transforms, combined with integration along a modified Bromwich contour in the complex plane, we finally obtain

$$\begin{aligned}
 W_{1,2}^{(h)} = & e^{-2\beta t} \int_0^t P_{1,2}(\xi) \exp[(2\beta - if)\xi - c^2/(4\nu_{1,2}\xi)] d\xi \\
 & + e^{-ift} \int_0^\infty [M(\xi) \cos(c\xi^{1/2}/\nu_{1,2}^{1/2}) + N_{1,2}(\xi) \sin(c\xi^{1/2}/\nu_{1,2}^{1/2})] \exp(-\xi t) d\xi.
 \end{aligned}
 \tag{A 1}$$

$$\left. \begin{aligned} \text{Here} \quad P_{1,2} &= \frac{1}{(\pi\xi)^{\frac{1}{2}}} \left[2k(2+Q-F_2)\nu_{\frac{1}{2}}^{\frac{1}{2}} + cK_{1,2} \frac{1+F_2-F_1}{2\xi\nu_{1,2}^{\frac{1}{2}}} \right], \\ M &= \frac{2k}{\pi\xi^{\frac{1}{2}}} \left[\theta \frac{(1-F_1)\nu_{\frac{1}{2}}^{\frac{1}{2}}}{\xi+4k^2\nu_1} + \frac{(1-F_2)\nu_{\frac{1}{2}}^{\frac{1}{2}}}{\xi+4k^2\nu_2} \right], \\ N_{1,2} &= \frac{K_{1,2}}{\pi} \left[\frac{1-F_1}{\xi+4k^2\nu_1} - \frac{1-F_2}{\xi+4k^2\nu_2} \right], \end{aligned} \right\} \quad (\text{A } 2)$$

$$\text{where} \quad K_1 = 1 \quad (\text{air, } c \geq 0); \quad K_2 = \theta \quad (\text{water, } c \leq 0). \quad (\text{A } 3)$$

F_1 and F_2 are given by (4.3). For a fuller account of the mathematical details connected with these calculations, reference is made to Førland (1989).

REFERENCES

- ANDREWS, D. G. & McINTYRE, M. E. 1978 An exact theory of nonlinear waves on a Lagrangian-mean flow. *J. Fluid Mech.* **89**, 609–646.
- BASSET, A. B. 1888 *Hydrodynamics*, vol. 2. Cambridge: Deighton and Bell.
- BYE, J. A. T. 1988 The coupling of wave drift and wind velocity profiles. *J. Mar. Res.* **46**, 457–472.
- CHANG, M.-S. 1969 Mass transport in deep-water long-crested random gravity waves. *J. Geophys. Res.* **74**, 1515–1536.
- CHEUNG, T. K. & STREET, R. L. 1988 The turbulent layer in the water at an air–water interface. *J. Fluid Mech.* **194**, 133–151.
- CHURCHILL, J. H. & CSANADY, G. T. 1983 Near-surface measurements of quasi-Lagrangian velocities in open water. *J. Phys. Oceanogr.* **13**, 1669–1680.
- CRAIK, A. D. D. 1982 The drift velocity of water waves. *J. Fluid Mech.* **116**, 187–205.
- DORE, B. D. 1978*a* Some effects of the air–water interface on gravity waves. *Geophys. Astrophys. Fluid Dyn.* **10**, 215–230.
- DORE, B. D. 1978*b* A double boundary-layer model of mass transport in progressive interfacial waves. *J. Engng Maths* **12**, 289–301.
- FØRLAND, E. 1989 Wave-induced currents in the ocean. Dr. Scient. dissertation, University of Oslo, Norway. 182 pp.
- GASTER, M. 1962 A note on the relation between temporally-increasing and spatially-increasing disturbances in hydrodynamic stability. *J. Fluid Mech.* **14**, 222–224.
- GRIMSHAW, R. 1981 Mean flows generated by a progressing water wave packet. *J. Austral. Math. Soc.* **B22**, 318–347.
- HASSELMANN, K. 1970 Wave-driven inertial oscillations. *Geophys. Fluid Dyn.* **1**, 463–502.
- JENKINS, A. D. 1986 A theory for steady and variable wind- and wave-induced currents. *J. Phys. Oceanogr.* **16**, 1370–1377.
- JENKINS, A. D. 1987 Wind and wave induced currents in a rotating sea with depth-varying eddy viscosity. *J. Phys. Oceanogr.* **17**, 938–951.
- LAMB, H. 1932 *Hydrodynamics*, 6th edn. Cambridge University Press.
- LONGUET-HIGGINS, M. S. 1953 Mass transport in water waves. *Phil. Trans. R. Soc. Lond.* **A245**, 535–581.
- LONGUET-HIGGINS, M. S. 1969 A nonlinear mechanism for the generation of sea waves. *Proc. R. Soc. Lond.* **A311**, 371–389.
- MADSEN, O. S. 1977 A realistic model of the wind-induced Ekman boundary layer. *J. Phys. Oceanogr.* **7**, 248–255.
- MCLEISH, W. L. & PUTLAND, G. E. 1975 Measurements of wind-driven flow profiles in the top millimeter of water. *J. Phys. Oceanogr.* **5**, 516–518.
- PHILLIPS, O. M. 1985 Spectral and statistical properties of the equilibrium range in wind-generated gravity waves. *J. Fluid Mech.* **156**, 505–531.

- PIERSON, W. J. 1962 Perturbation analysis of the Navier–Stokes equations in Lagrangian form with selected linear solutions. *J. Geophys. Res.* **67**, 3151–3160.
- POLLARD, R. T. 1970 Surface waves with rotation: An exact solution. *J. Geophys. Res.* **75**, 5895–5898.
- SHEMDIN, O. H. 1972 Wind-generated current and phase speed of wind waves. *J. Phys. Oceanogr.* **2**, 411–419.
- STOKES, G. G. 1847 On the theory of oscillatory waves. *Trans. Camb. Phil. Soc.* **8**, 441–455.
- WEBER, J. E. 1983*a* Attenuated wave-induced drift in a viscous rotating ocean. *J. Fluid Mech.* **137**, 115–129 (referred to as (I) herein).
- WEBER, J. E. 1983*b* Steady wind- and wave-induced currents in the open ocean. *J. Phys. Oceanogr.* **13**, 524–530.
- WEBER, J. E. 1987 Wave attenuation and wave drift in the marginal ice zone. *J. Phys. Oceanogr.* **17**, 2351–2361.
- WEBER, J. E. 1989 Eulerian versus Lagrangian approach to wave drift in a rotating ocean. *Vetenskaps och Vitterhetssamhället, Göteborg, Acta: Geophys.* **4**, (in press).
- WEBER, J. E. & FØRLAND, E. 1989 Effect of an insoluble surface film on the drift velocity of capillary-gravity waves. *J. Phys. Oceanogr.* **19**, 952–961.
- WU, J. 1975 Wind-induced drift currents. *J. Fluid Mech.* **68**, 49–70.
- WU, J. 1982 Wind-stress coefficients over sea surface from breeze to hurricane. *J. Geophys. Res.* **87**, 9704–9706.